Journal of Orthopaedic Translation 44 (2024) 114–124

Contents lists available at ScienceDirect

Journal of Orthopaedic Translation

journal homepage: www.journals.elsevier.com/journal-of-orthopaedic-translation

XJB-5-131 protects chondrocytes from ferroptosis to alleviate osteoarthritis progression via restoring Pebp1 expression☆

Wei Sun [a,b,d,1], Zhongyang Lv [c,1], Weitong Li [e,1], Jun Lu [b], Ya Xie [e], Peng Wang [b], Ruiyang Jiang [f], Jian Dong [b], Hu Guo [b], Zizheng Liu [b], Yuxiang Fei [b], Guihua Tan [b], Maochun Wang [b], Kewei Ren [a], Jun Xu [a], Huiqing Sun [a], Xuefeng Jiang [a,d,**], Dongquan Shi [b,e,f,*]

[a] Department of Orthopedics, Jiangyin People's Hospital Affiliated to Nantong University, 163 Shoushan Road, Jiangyin, 214400, Jiangsu, PR China
[b] State Key Laboratory of Pharmaceutical Biotechnology, Division of Sports Medicine and Adult Reconstructive Surgery, Department of Orthopedic Surgery, Affiliated Drum Tower Hospital, Medical School, Nanjing University, 321 Zhongshan Road, Nanjing, 210008, Jiangsu, PR China
[c] Department of Orthopedics, Nanjing Jinling Hospital, Affiliated Hospital of Medical School, Nanjing University, Nanjing, PR China
[d] Department of Orthopedics, The Jiangyin Clinical College of Xuzhou Medical University, 163 Shoushan Road, Jiangyin, 214400, Jiangsu, PR China
[e] Nanjing Drum Tower Hospital Clinical College of Traditional Chinese and Western Medicine, Nanjing University of Chinese Medicine, Nanjing, 210008, Jiangsu, PR China
[f] Nanjing Drum Tower Hospital Clinical College of Xuzhou Medical University, Xuzhou Medical University, Nanjing, 210008, Jiangsu, PR China

ARTICLE INFO

Keywords:
Cartilage degeneration
Ferroptosis
Osteoarthritis
XJB-5-131

ABSTRACT

Background: Osteoarthritis (OA) is the most common age-related musculoskeletal disease. However, there is still a lack of therapy that can modify OA progression due to the complex pathogenic mechanisms. The aim of the study was to explore the role and mechanism of XJB-5-131 inhibiting chondrocytes ferroptosis to alleviate OA progression.

Methods: We treated tert-butyl hydroperoxide (TBHP)-induced ferroptosis of mouse primary chondrocytes with XJB-5-131 in vitro. The intracellular ferroptotic hallmarks, cartilage anabolic and catabolic markers, ferroptosis regulatory genes and proteins were detected. Then we established a mouse OA model via destabilization of the medial meniscus (DMM) surgery. The OA mice were treated with intra-articular injection of XJB-5-131 regularly (2 μM, 3 times per week). After 4 and 8 weeks, we performed micro-CT and histological examination to evaluate the protection role of XJB-5-131 in mouse OA subjects. RNA sequencing analysis was performed to unveil the key downstream gene of XJB-5-131 exerting the anti-ferroptotic effect in OA.

Results: XJB-5-131 significantly suppressed TBHP-induced increases of ferroptotic hallmarks (ROS, lipid peroxidation, and Fe^{2+} accumulation), ferroptotic drivers (Ptgs2, Pgd, Tfrc, Atf3, Cdo1), while restored the expression of ferroptotic suppressors (Gpx4, Fth1). XJB-5-131 evidently promoted the expression of cartilage anabolic and decreased the expression of cartilage catabolic markers. Moreover, intra-articular injection of XJB-5-131 significantly inhibited the expression of Cox2 and Mmp13, while promoted the expression of Col2a1, Gpx4 and Fth1 in DMM-induced mouse articular cartilage. Further, we identified Pebp1 as a potential target of XJB-5-131 by RNA sequencing analysis. The anti-ferroptosis and chondroprotective effects of XJB-5-131 were significantly diminished by Locostatin, a specific antagonist of Pebp1.

☆ All authors have read and approved the manuscript and agreed to be accountable for all aspects of the work.

* Corresponding author. Department of Sports Medicine and Adult Reconstructive Surgery, Nanjing Drum Tower Hospital, The Affiliated Hospital of Nanjing University Medical School, 321 Zhongshan Road, Nanjing, 210008, Jiangsu, PR China.

** Corresponding author. Department of Orthopedic, Jiangyin People's Hospital Affiliated to Nantong University, 163 Shoushan Road, Jiangyin, 214400, Jiangsu, PR China.

E-mail addresses: Sunw1988@outlook.com (W. Sun), zhongyanglv@163.com (Z. Lv), 1554845347@qq.com (W. Li), 540936052@qq.com (J. Lu), 459895571@qq.com (Y. Xie), 15850681759@163.com (P. Wang), jry1028@163.com (R. Jiang), jiandong@alumni.hust.edu.cn (J. Dong), 15050583626@163.com (H. Guo), liuzizheng2020@163.com (Z. Liu), 975778674@qq.com (Y. Fei), gwennethgh@163.com (G. Tan), wangmaochun0815@163.com (M. Wang), Keweiren@hotmail.com (K. Ren), xj6520@sina.com (J. Xu), hqsuntd@foxmail.com (H. Sun), jxfeng18@hotmail.com (X. Jiang), shidongquan@nju.edu.cn (D. Shi).

[1] These authors contributed equally to this work.

https://doi.org/10.1016/j.jot.2023.12.005
Received 7 June 2023; Received in revised form 30 December 2023; Accepted 30 December 2023

Conclusion: XJB-5-131 significantly protects chondrocytes from ferroptosis in TBHP-induced mouse primary chondrocytes and DMM surgery-induced OA mice model via restoring the expression of Pebp1. XJB-5-131 is a potential therapeutic drug in the management of OA progression.

The translational potential of this article

We demonstrate that XJB-5-131 is a potential therapeutic drug in the management of OA, which provides a new breakthrough in the mechanism treatment of OA with clinical potential.

1. Introduction

Osteoarthritis (OA) is the most prevalent age-related musculoskeletal disease characterized by swelling and pain of involved joints, which can be accompanied by joint deformity, movement limitation, and even disability in severe cases [1–4]. Although OA has been recognized for a long time, however, there is still a lack of therapy modifying its progression due to the complex pathogenic mechanisms. The U.S. Food and Drug Administration (FDA) classified OA as "a serious disease with unmet medical need" [5]. There was an urgent need to develop new drugs for the treatment of OA.

Cartilage degeneration has been recognized as the main pathogenesis of OA progression, in which injury of chondrocytes, the only one cell type in cartilage, directly accelerated this process [6–8]. Multiple types of chondrocyte death have been identified in cartilage degeneration [8,9]. Recently, chondrocyte ferroptosis has been suggested to be direct-ly involved in OA cartilage degeneration [10]. Ferroptosis is a novel form of iron-dependent programmed cell death characterized by lipid peroxidation, accumulated ferrous ions, and depleted glutathione, which is significantly different from previously identified programmed cell death at the genetic, morphological, and biological levels [11–13]. Increasing studies focused on chondrocyte ferroptosis in OA [14–17], whereas, few investigations have been reported to inhibit chondrocyte ferroptosis and alleviate OA. The nitroxide XJB-5-131 is an antioxidant targeting mitochondria and has achieved satisfactory efficacy in a variety of diseases [18–23], as well as being considered a potential inhibitor of ferroptosis [24]. However, the role and mechanism of XJB-5-131 in OA progression have not been investigated.

In the current study, we explored the anti-ferroptotic effects of XJB-5-131 with primary mouse chondrocytes and mouse OA model induced by destabilization of the medial meniscus (DMM) surgery. We found that XJB-5-131 exhibited anti-ferroptotic effect of chondrocyte and alleviated OA progression. These results have important implications for the development of novel therapeutic agents based on the pathogenesis of OA.

2. Materials and methods

2.1. Ethics statement

All experimental procedures were in accordance with the Declaration of Helsinki. The animal experimental procedures were performed in strict accordance with the guidelines of the Animal Care and Use Committee of Nanjing Drum Tower Hospital (2020AE01102).

2.2. Isolation and culture of mouse primary chondrocytes

The murine primary chondrocytes were isolated and cultured referring to previous protocols [25]. Briefly, the cartilage tissues from the 3-day-old C57BL/6 mice (purchased from Model Animal Research Center of Nanjing University) were digested in 0.2 % type II collagenase (Gibco, USA) at 37 °C) for 4 h. After removing soft tissues and filtrating with a cell strainer (Corning, USA), the isolated chondrocytes were cultured in Dulbecco's modified Eagle's medium contained 1 g/L glucose (DMEM/F12) (Gibco, USA) supplemented with 1 % penicillin–streptomycin (Invitrogen, USA) and 10 % fetal bovine serum (Gibco, USA) in the incubator (5 % CO2, 37 °C) (Thermo Scientific, USA). The cell culture medium was refreshed every 48 h, and chondrocytes from passages 1 to 3 were used in cell experiments.

2.3. Cell viability assay

To assess the cytotoxicity of tert-butyl hydroperoxide (TBHP) (#MKCH9944, Sigma, USA) to chondrocytes in the presence or absence of XJB-5-131 (#SML2982, Sigma, USA), CCK-8 assay was performed (#CK04, Dojindo, Japan) according to the manufacturer's instruction. Uniformly chondrocytes were seeded in 96-well plates and cultured with TBHP and/or XJB-5-131 for 24 h. After washed by PBS, the cells were then incubated with DMEM/F12 containing 10 % CCK-8 solution for 90min at 37 °C. The OD values were measured at 450 nm with a microplate reader (Thermo Scientific, USA).

2.4. Quantitative real-time PCR

The cellular mRNA isolation and qPCR were performed essentially using RNA-quick Purification Kit (#RN001, ES Science, Shanghai, China), HiScript-TS 5'/3′ RACE Kit (RA101, Vazyme Biotech Co.,Ltd, China) and ChamQ™ SYBR Color qPCR Master Mix (Q411, Vazyme, China) according to previous protocols [26]. The primer sequences used were as follows:

Gapdh: 5' – AGGTCGGTGTGAACGGATTTG- 3' (forward)
and 5' – TGTAGACCATGTAGTTGAGGTCA- 3' (reverse)
Atf3: 5' – GAGGATTTTGCTAACCTGACACC- 3' (forward)
and 5' – TTGACGGTAACTGACTCCAGC- 3' (reverse)
Gpx4: 5' – TGTGCATCCCGCGATGATT- 3' (forward)
and 5' – CCCTGTACTTATCCAGGCAGA- 3' (reverse)
Pgd: 5' – TGAAGGGTCCTAAGGTGGTCC- 3' (forward)
and 5' – CCGCCATAATTGAGGGTCCAG- 3' (reverse)
Cdo1:5' – GGGGACGAAGTCAACGTGG- 3' (forward)
and 5' – ACCCCAGCACAGAATCATCAG- 3' (reverse)
Ptgs2: 5' – TGAGCAACTATTCCAAACCAGC- 3' (forward)
and 5' – GCACGTAGTCTTCGATCACTATC- 3' (reverse)
Col2a1: 5' – CCAGATGACCTTCCTACGCC- 3' (forward)
and 5' – TTCAGGGCAGTGTACGTGAAC- 3' (reverse)
Acan: 5' – GTGCCTATCAGGACAAGGTCT- 3' (forward)
and 5' – GATGCCTTTCACCACGACTTC- 3' (reverse)
Mmp13: 5' – TCTTTATGGTCCAGGCGATGA- 3' (forward)
and 5' – ATCAAGGGATAGGGCTGGGT- 3' (reverse)
Mmp3: 5' – ATGGGCCTGGAACAGTCTTG- 3' (forward)
and 5' – GTGGGAGTTCCATAGAGGGAC- 3' (reverse)
Tfrc: 5' – GTTTCTGCCAGCCCCTTATTAT- 3' (forward)
and 5' – GCAAGGAAAGGATATGCAGCA- 3' (reverse)

2.5. Intracellular Fe^{2+}, ROS and lipid peroxidation detection

Intracellular levels of ferrous iron (Fe^{2+}), ROS and lipid peroxidation were measured with Flow Cytometry as previously described [15]. Briefly, chondrocytes were incubated with 1 μM Fe^{2+} probe FerroOrange (#F374, Dojindo, Japan), 10 μM ROS probe DCFH-DA (#S0033S, beyotime, China) and 5 μM lipid ROS probe C11-BODIPY (#GC40165, GLPBIO, USA) for 40 min in the incubator (37 °C, 5 % CO2), respectively. After washing the probes with PBS, the chondrocytes were treated with 50 μM TBHP and/or 2 μM XJB-5-131, 10 μM Locostatin (#A16079, Adooq, China) for 4 h. Then the fluorescent intensity of

chondrocytes was measured by Flow Cytometry (BD Biosciences, USA). FlowJo software (Version 10, USA) was used to analyzed the data.

2.6. Protein extraction and western blot

The total protein of chondrocytes with different treatment were extracted using a whole Cell Lysis Assay Kit (#KGA1202, Keygen, China). Protein concentration measurements and western blot were performed according to the previously described protocols [26]. The primary antibodies used were as follows: anti-Collage II (#BA0533, Boster, China), anti-MMP13 ((#ab219620, Abam, UK), anti-Cox2 (#66351-1-Ig, Proteintech, China), anti-FTH1 (#4393, Cell Signaling Technology, USA), anti-GPX4 (#ab125066, Abam, UK), anti-PEBP1 (#GB113118, Servicebio, China). After HRP-conjugated goat anti-rabbit/mouse secondary antibodies (#BL003A or #BL001A, Biosharp, China) incubation, an ECL Western Blot Kit (Tanon, China) was used to detect signals. Finally, we quantified the protein bands with Image J software (version 1.8.0, USA).

2.7. Animals study

Twelve weeks old wild-type C57BL/6 male mice were purchased from the Model Animal Research Center of Nanjing University, and acclimated in specific pathogenfree (SPF) condition. The mice were randomly divided into the following 4 groups: (1) Sham operation (Sham); (2) Sham operation with XJB-5-131 treatment (XJB); (3) Destabilization of medial meniscus (DMM); and (4) DMM with XJB-5-131 treatment (DMM + XJB). The XJB-5-131 (2 μM, 8 μl, 3 times/week) was intra-articularly injected into the right knees since 1 week after DMM surgery for 4 W or 8 W. The equal volume of saline was injected in the Sham and DMM groups. The DMM procedure were performed as previouly decribed [26].

2.8. Micro-CT analysis

Mouse knee joints were fixed in 4 % paraformaldehyde (PFA), and then were evaluated with a micro-CT scanner (mCT80, Scanco Medical AG, Switzerland). As previously de-scribed. We analyzed the images and reconstructed the 3D knee joints with Scanco Medical software. The number of osteophytes, subchondral plate thickness (SBP), bone volume (BV), subchondral bone mineral density (BMD), bone volume/tissue volume (BV/TV), trabecular thickness (Tb.Th), trabecular separation (Tb.Sp), trabecular number (Tb.N) were acquired from the Scanco Medical software.

2.9. Histological analysis

After treatment, the experimental knee joints were surgically removed and fixed in 4 % PFA, decalcified with 10 % EDTA and embedded in paraffin. The subjects were sliced into continuous coronal 5 μm slides by a microtome (Thermo, USA) and stained with safranin O/fast green (Solarbio, China). The Osteoarthritis Research Society International (OARSI) grading system was used to evaluate the cartilage destruction. We also analyzed the thickness of cartilage and the number of chondrocytes.

2.10. Immunofluorescence staining

After dewaxing, the histological sections of mouse knee joints were blocked with 5 % bovine serum albumin (BSA) for 1 h at room temperature, then incubated overnight at 4 °C with primary antibodies as follows: anti-Collage II (#BA0533, Boster, China), an-ti-MMP13 (#ab219620, Abam, UK), anti-Cox2 (#ab219620, Abam, UK). Then, the slides were washed with TBST and incubated with a fluorescein-conjugated secondary antibody (#BL003A or #BL001A, Abcam, USA) for 60 min at room temperature. Then we stained the nuclei with DAPI (#SC3598, Santa Cruz, USA). A fluorescence microscope (Zeiss, Germany) was used to observe and acquire the images.

2.11. RNA sequence analysis

Total RNA was extracted from primary chondrocytes after the treatment of TBHP with or without XJB-5-131 for 6 h (n = 3). The RNA was submitted to GeneChem company (Shanghai, China) for RNA sequencing analysis. The Pearson's correlation analysis and heatmaps were performed. In this study, differentially expressed genes (DEGs) were defined as fold changes >2 and $P < 0.05$. We used Gene ontology (GO) and Kyoto Encyclopedia of Genes and Genomes (KEGG) analysis to assess the biological function of DEGs.

2.12. Statistical analysis

The data were expressed as the mean ± standard deviation (S.D.). The data were statistically analyzed by GraphPad Prism software (version 8.0, USA) and SPSS software (version 24.0, USA). The quantitative data used represent the results of no less than three independent repeated experiments. Levene method and Shapiro–Wilk test were used for the estimation of data homogeneity of variance and normal distribution, respectively. The data between two groups were compared with unpaired two-tailed t-test. When more than 2 groups, we performed One-way ANOVA statistical analysis. The statistically significant was considered as $P < 0.05$.

3. Results

3.1. XJB-5-131 suppresses TBHP-induced chondrocytes ferropotsis in vitro

The cytotoxicity of XJB-5-131 were performed by CCK-8 kit, the results showed that XJB-5-131 at concentrations of 0.1–5 μM exhibited no cytotoxic effects on chondrocyte viability while reduced chondrocyte viability but had no significant difference at 5 μM concentration. As previously described, we used tert-butyl hydroperoxide (TBHP) (50 μM) to induce mouse primary chondrocyte ferropotsis in vitro [15]. The viability of chondrocytes was significantly decreased after 12 h incubation of TBHP, however, the cytotoxicity was significantly alleviated when the concentration of XJB-5-131 increased (Fig. 1A). Next, we found that XJB-5-131 significantly alleviated the ferroptotic hallmarks (intracellular ROS level, Fe^{2+} accumulation and lipid peroxidation level) in TBHP-induced chondrocytes by flow cytometry (Fig. 1B). Q-PCR verified that XJB-5-131 promoted the expression of chondrocyte anabolic genes (Col2a1 and Acan) and inhibited chondrocyte catabolic genes (Mmp13 and Mmp3) (Fig. 1C). In addition, under the treatment of TBHP, the ferroptotic suppressor (Gpx4) was evidently up-regulated and ferroptotic drivers (Tfrc, Atf3, Ptgs2, Cdo1, Pgd) were significantly down-regulated by XJB-5-131(Fig. 1C). Moreover, western blot analysis showed that XJB-5-131 significantly promoted the expression of chondrocyte anabolic protein (Col2a1) and ferroptotic suppressors (Gpx4 and Fth1), while markedly decreased chondrocyte metabolic protein (Mmp13) and ferroptotic driver (Cox2) (Fig. 1D). These results suggest that XJB-5-131 plays an anti-ferroptotic role in chondrocytes.

3.2. XJB-5-131 alleviates DMM-induced osteophyte formation and subchondral bone sclerosis

To gain insight into whether XJB-5-131 can suppress chondrocyte ferroptosis and alleviate OA in vivo, we performed intra-articular injection of XJB-5-131 in the OA mouse model. Previous study suggested that OA cartilage degeneration was highly associated with bone redundancy formation and subchondral bone microarchitectural changes [27]. We further analyzed the effect of XJB-5-131 on the bone quality of the mice knee joint. We found osteophytes, subchondral bone

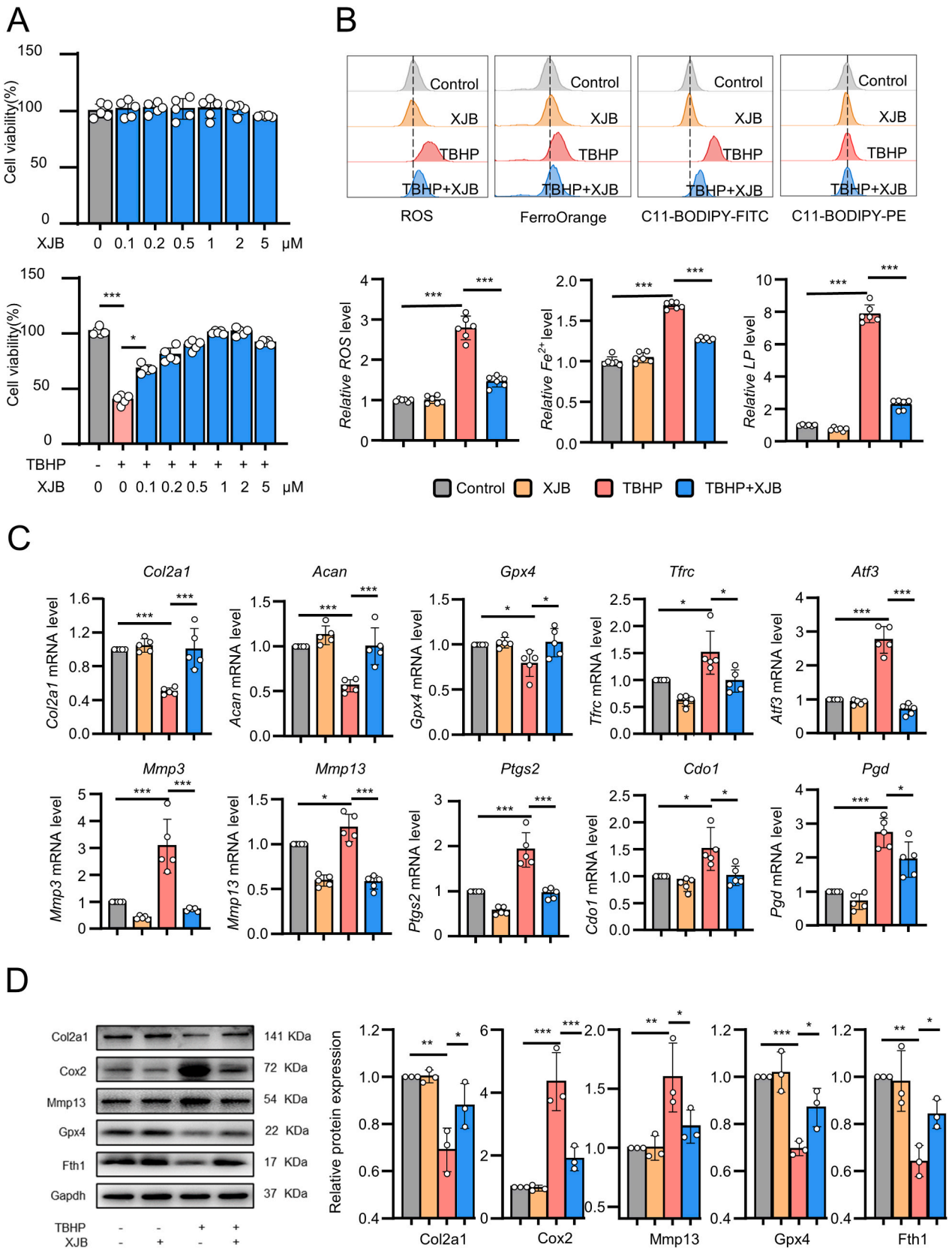

Fig. 1. XJB-5-131 suppresses TBHP-induced chondrocytes ferropotsis in vitro. (A) The viability of primary chondrocytes after XJB-5-131 treatment with or without TBHP(n = 5). (B) Flow cytometry analysis and quantitative analysis of intracellular total reactive oxygen species (ROS), FerroOrange (Fe^{2+}), lipid peroxidation (C11-BODIPY) (n = 6). (C) Q-PCR analysis of indicated genes in chondrocytes treated with 50 μM TBHP and/or 2 μM XJB-5-131 for 6 h (n = 5). (D)Western blot analysis of protein expression and quantification of Col2a1, Cox2, MMP13, Fth1 and Gpx4 in chondrocytes treated with XJB-5-131 (2 μM) with or without TBHP(n = 3). The values are presented as the means ± SDs. *P < 0.05; **P < 0.01; ***P < 0.001.

thickness increased significantly in the knee joint of DMM mice with micro-CT both in 4 weeks and 8 weeks group (Fig. 2A–C). In 4 weeks group, we found the bone volume (BV), subchondral bone mineral density (BMD), bone volume/tissue volume (BV/TV), subchondral trabecular thickness (Tb.Th), the number of osteophyte and subchondral bone plate(SBP) thickness were significantly higher in the DMM mice, while the subchondral trabecular separation(Tb.Sp) significantly reduced and trabecular number (Tb.N) showed no significant change (Fig. 2A). Intra-articular administration of XJB-5-131 significantly alleviate osteophyte formation and subchondral bone thickness (Fig. 2B). The trend of these index in 8 weeks group were similar to that in 4 weeks group and the effect of XJB-5-131 was more pronounced than that in 4 weeks (Fig. 2D). These results suggest that XJB-5-131 suppresses the osteophyte formation and subchondral bone sclerosis in

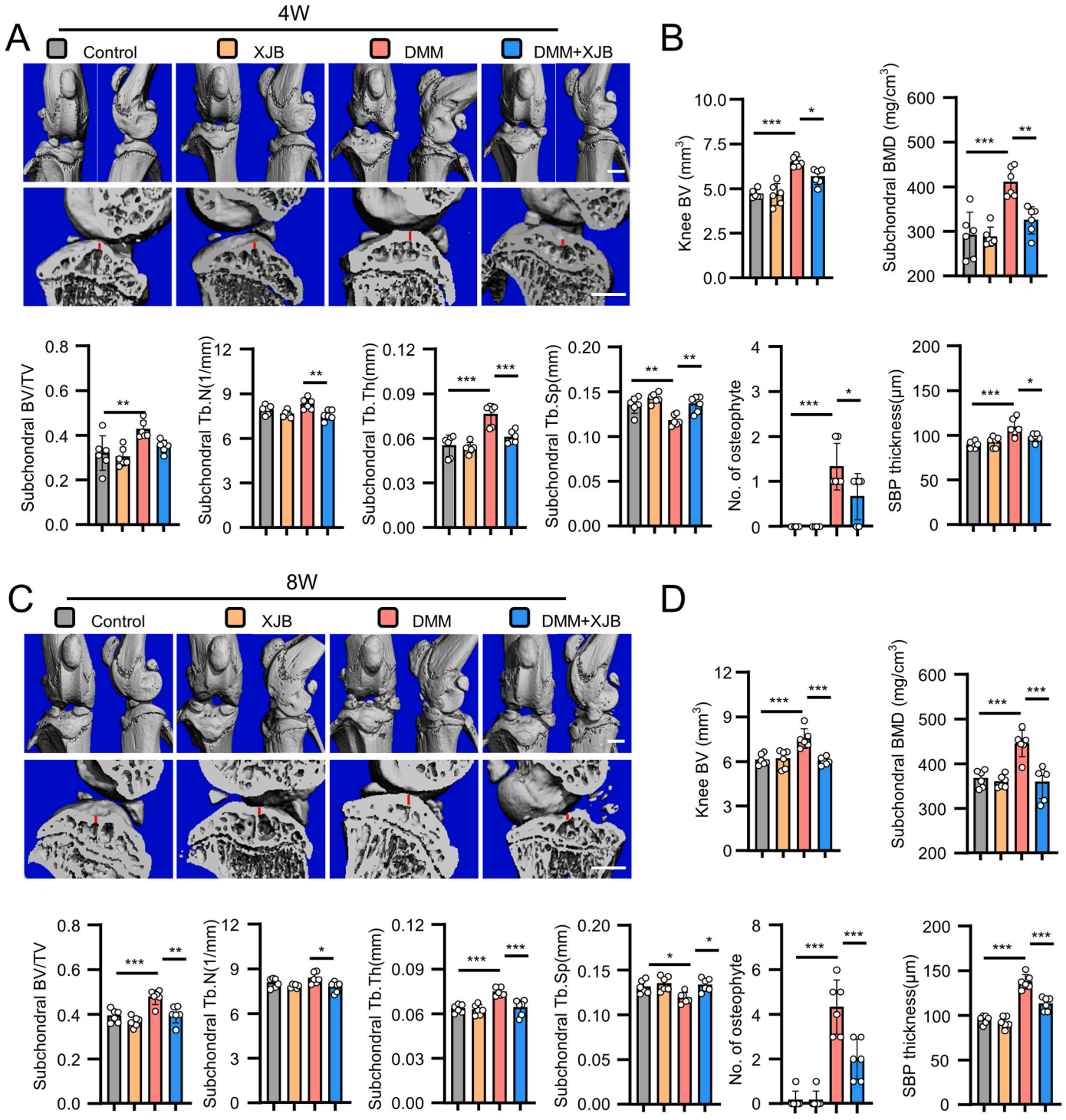

Fig. 2. XJB-5-131 alleviates DMM-induced bone redundancy formation and subchondral bone microarchitectural changes. (A, C) 3D reconstructed images of mice knee joints and the sagittal view of the medial joint compartment revealing the changes to femoral and tibial surfaces and subchondral bone plate (SBP) thickness, respectively. Red line indicates the thickness of SBP (4 weeks and 8 weeks, n = 6). (B, D) Micro-CT analysis of indicated markers of bone redundancy formation and subchondral bone microarchitectural changes (4 weeks and 8 weeks, n = 6). Scale bars, 1 mm (A, C) The values are presented as the means ± SDs. *P < 0.05; **P < 0.01; ***P < 0.001.

DMM-induced mice OA model.

3.3. XJB-5-131 alleviates OA progression via inhibiting chondrocytes ferroptosis

Next, we performed safranin O/fast green staining of mice joints and found decreased cartilage thickness, reduced chondrocytes numbers, and increased OARSI scores in the DMM mice compared to the Sham mice in both 4 weeks and 8 weeks group, which were significantly alleviated by the intra-articular injection of XJB-5-131 (Fig. 3A–D). To further evaluate the anti-ferroptotic and chondroprotective effects of XJB-5-131, we performed immunofluorescence staining of mice articular cartilage. The histological examination revealed reduced Col2a1, Fth1 and Gpx4 expression, whereas increased Mmp13 and Cox2 expression in DMM-induced mice cartilage, which were markedly abolished by XJB-5-131 treatment both in 4 weeks and 8 weeks group (Fig. 3E–G). Taken together, these data indicates that XJB-5-131 inhibits DMM-induced articular cartilage erosion and chondrocyte ferroptosis.

3.4. Pebp1 is a potential mediator of XJB-5-131 exerting the anti-ferroptotic effect in chondrocytes

To explore the mechanisms of XJB-5-131 inhibiting chondrocytes ferroptosis, we performed RNA sequencing analysis of mouse chondrocytes treated with TBHP in the presence or absence of XJB-5-131. Compared with control group, there were 8361 DEGs in TBHP group, within which 4239 genes were up-regulated and 4122 were down-regulated. Moreover, compared with the TBHP group, there were 5500 differentially expressed genes in the TBHP + XJB-5-131 group, of which 2567 were up-regulated and 2933 were down-regulated (Fig. 4A). There were 3870 common difference genes between Control group vs TBHP group and TBHP group vs TBHP + XJB-5-131 group (Fig. 4B). Compared with the Control group, the GO in TBHP group was significantly enriched ROS metabolic processes, cellular transition metal ion homeostasis and regulation of membrane lipid distribution (Fig. 4C). Furthermore, the cellular iron ion homeostasis and glutathione peroxidase activity were more enriched while the ROS metabolic processes were less enriched in the TBHP + XJB group than the TBHP group (Fig. 4C). All of these reveals that XJB-5-131 significantly suppressed TBHP induced chondrocyte ferroptosis.

Within the heat map of DEGs, we noted that the Pebp1 was significantly down-regulated after TBHP treatment and was restored by XJB-5-131 (Fig. 4D). Therefore, we speculated that Pebp1 may be an important mediator of XJB-5-131 resistance to chondrocyte ferroptosis. Then, we performed immunofluorescence staining of mice knee sections to verify the expression of Pebp1 protein in cartilage. Both in 4 weeks and 8 weeks groups, the Pebp1 were significantly decreased in the DMM mice while XJB-5-131 treatment evidently restored its expression (Fig. 4E). Taken together, these results suggest that Pebp1 is a potential target of XJB-5-131 exerting anti-ferroptotic effects in chondrocytes.

3.5. Inhibition of pebp1 disables the effect of xjb-5-131 resistant to chondrocyte ferroptosis

Pebp1 was a small hybrid scaffold protein, which was bound to and inhibited the Raf1 kinase cascade under homeostatic conditions, therefore, Pebp1 was also known as Raf1 kinase inhibitory protein (RKIP) [28]. Locostatin, a Pebp1 specific inhibitor, disrupted the interaction of Pebp1 and Raf1 kinase and liberated Pebp1 by binding 15LO [29,30]. We selected Locostatin as an inhibitor of Pebp1 to explore the mechanism of Pebp1 in XJB-5-131 against chondrocyte ferroptosis. We treated primary chondrocytes with different concentrations of Locostatin for 24 h and revealed no significant effect on chondrocyte viability at 5 and 10 μM. In contrast, the same concentration of Locostatin blocked XJB-5-131 from rescuing the TBHP induced chondrocyte toxicity (Fig. 5A). Next, we found Locostatin (10 μM) attenuates the beneficial effects of XJB-5-131 on alleviating the ferroptotic hallmarks with flow cytometry (Fig. 5B). Furthermore, Locostatin counteracted XJB-5-131's restoration of cartilage anabolic genes (Col2a1, Acan) and ferroptosis suppressor gene (Gpx4) as well as inhibition of cartilage catabolic genes (Mmp3, Mmp13) and ferroptosis drivers (Atf3, Ptgs2). In addition, the Pebp1 expression was decreased significantly after Locostatin treatment (Fig. 5C). Furthermore, similar results of cartilage metabolic, ferroptosis markers, and Pebp1 were also observed by western blot analysis (Fig. 5D). These results indicates that inhibition of Pebp1 disables the effect of XJB-5-131 resistance to chondrocyte ferroptosis.

4. Discussion

In this study, we explored the effect of XJB-5-131 in inhibiting chondrocyte ferroptosis and alleviating OA progression. There were several novel and important findings here: (1) XJB-5-131 significantly alleviated chondrocyte ferroptosis and restored cartilage metabolic homeostasis in vitro; (2) XJB-5-131 alleviated articular cartilage degeneration in DMM surgery induced OA mice model by suppressing chondrocyte ferroptosis; (3) XJB-5-131 exerted anti-ferroptotic effect on chondrocytes by restoring Pebp1 expression.

Recent studies have shown that ferroptosis plays an important role in the pathogenesis of various diseases, including OA [31–34]. Iron was not only an essential trace element in human body, but also indispensable for metabolic reactions in chondrocytes, such as redox reactions, cellular respiration and DNA synthesis [35,36]. However, the range of cellular benefits of iron was narrow, and intracellular iron overload in chondrocytes had been suggested as a risk factor for OA [37]. Iron in cells was mainly stored in ferritin, which consists of two types, ferritin heavy polypeptide 1 (Fth1) and ferritin light polypeptide 1 (Ftl1), in which Fth1 played the main role of iron storage [38]. Studies showed that Fth1 reduction would lead to the accumulation of Fe^{2+} and subsequent Fenton reactions, which would trigger ferroptosis. Conversely, increased Fth1 inhibited ferroptosis [39–41]. After treatment of XJB-5-131, the expression of Fth1 and Gpx4 increased while the ferroptosis driver Cox2 decreased significantly in primary chondrocytes. In the animal study, we could not obtain chondrocytes and use probes to detect the biochemical markers (ROS levels and lipid peroxidation) of ferroptosis of chondrocytes directly because various factors including temperature and digestive enzymes would interference the chondrocytes state during the process of cartilage acquisition, resulting in unreliable results. Therefore, immunofluorescence assay was used to measure the markers of cartilage synthesis and catabolism as well as ferroptosis to evaluate the anti-ferroptotic role and cartilage protective effect of XJB-5-131.

We screened and verified Pebp1 as a potential mediator of XJB-5-131 resistance to ferroptosis with RNA sequencing analysis and histological studies. Pebp1 was suggested as a key factor in the regulation of ferroptosis by binding with 15-lipoxygenase (15LOX) to form 15LOX/Pebp1 complex [42–45]. Wenzel et al. suggested that Locostatin disrupted the binding of Pebp1 to Raf1, and liberated it to form 15LOX/-Pebp1 complex to exacerbate ferroptosis [42]. In our study, the anti-ferroptotic effect of XJB-5-131 was significantly inhibited by Locostatin. XJB-5-131 protects chondrocytes from ferroptosis by restoring Pebp1 expression, and its inhibition will lead to the failure of XJB-5-131 treatment.

A growing number of studies have targeted the inhibition of chondrocyte ferroptosis since it was found to be involved in the progression of osteoarthritis [10,46,47]. However, there was few studies on targeting mitochondria to inhibit chondrocyte ferroptosis. The function of mitochondria in ferroptosis has been extensively studied, the main opinion was that mitochondria was important source of ROS involved in ferroptosis [48]. Moreover, ROS would lead to mitochondrial membrane lipid peroxidation [49,50]. The mitochondria-targeted antioxidant XJB-5-131 exhibited a potent anti-ferroptotic effect in cardiac cells and tubular epithelial cells [23,51]. Our investigation directly revealed that XJB-5-131 could alleviate OA progression by inhibiting chondrocyte

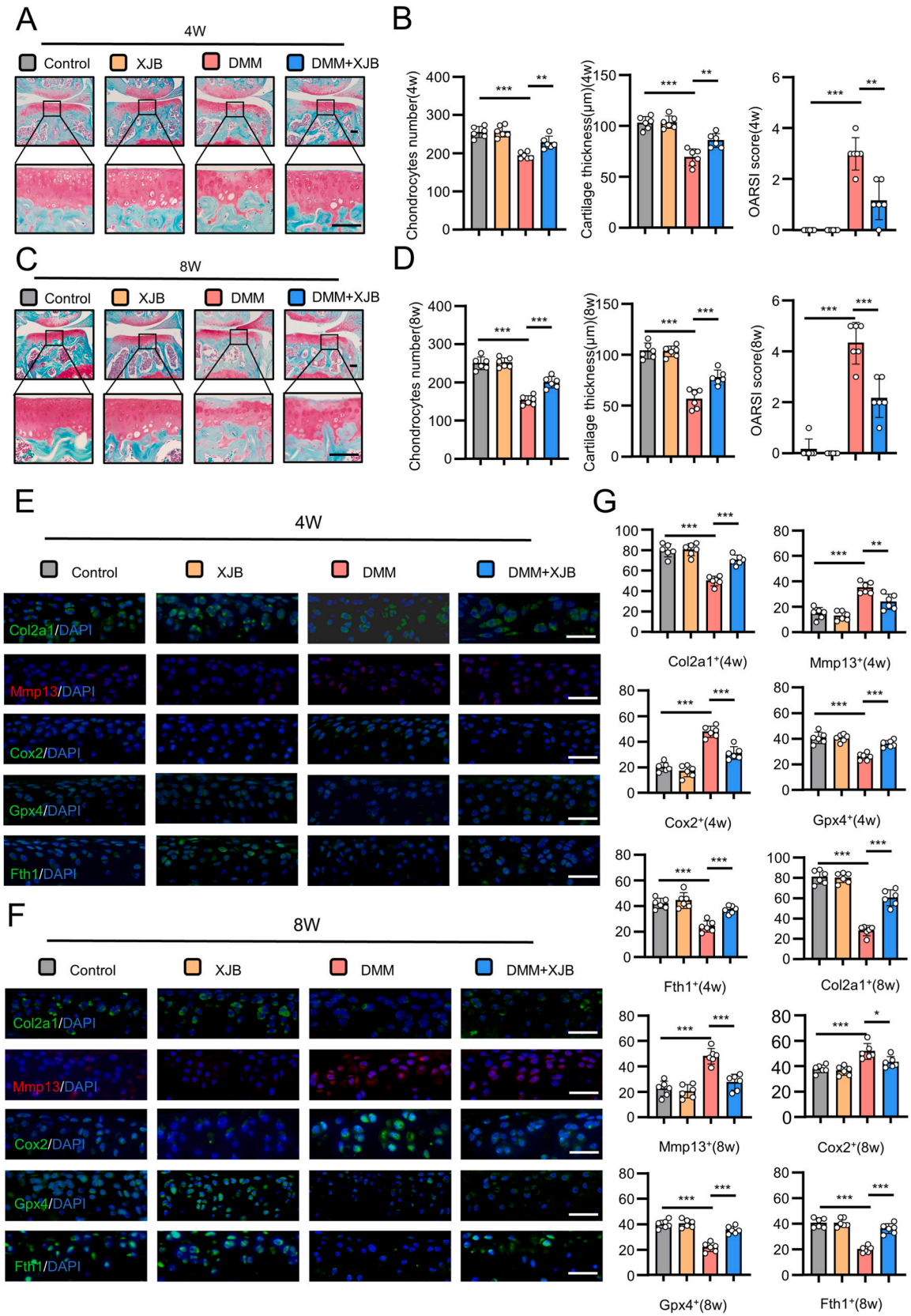

Fig. 3. XJB-5-131 ameliorates DMM-induced cartilage erosion chondrocyte ferropotsis in mouse knee joints. (A, C) Representative images of safranin-O/fast green stained knee joint sections in different groups (4 weeks and 8 weeks). (B, D) Quantitation of chondrocytes numbers, cartilage thickness and Osteoarthritis Research Society International (OARSI) scores (4 weeks and 8 weeks, n = 6). (E, F) IF staining of Col2a1, Mmp13, Cox2, Fth1, Gpx4 and their quantification (G) in different mice groups (4 weeks and 8 weeks, n = 6). Scale bars, 50 μm (A) (C) (E) (F), The values are presented as the means ± SDs. *P < 0.05; **P < 0.01; ***P < 0.001.

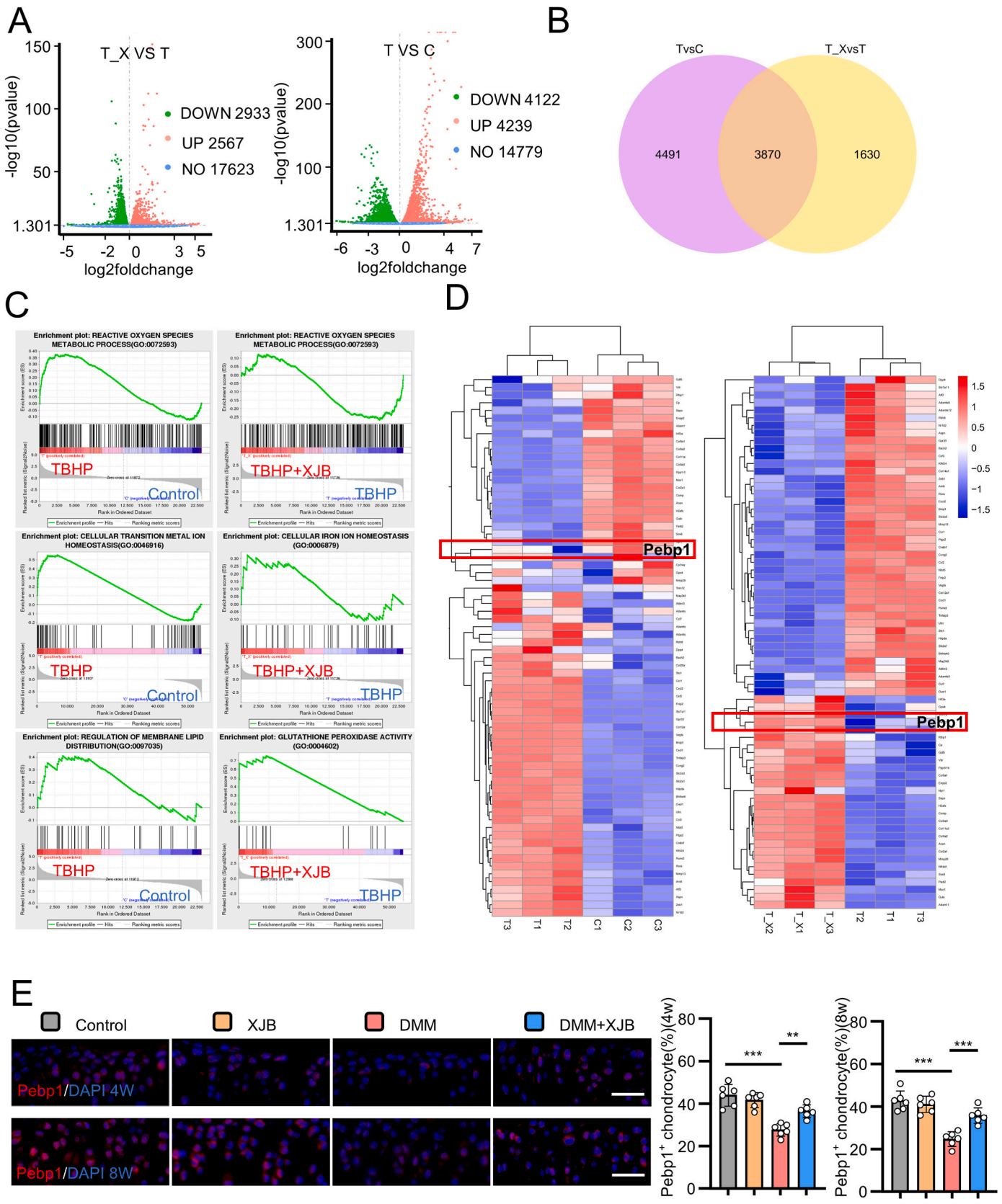

Fig. 4. RNA sequencing analysis of primary chondrocytes treated with TBHP in the presence or absence of XJB-5-131, which identified Pebp1 as a potential mediator of XJB-5-131 exerting the anti-ferroptosis in chondrocytes. (A) RNA sequencing Volcano Plot between TBHP group (T) vs TBHP + XJB-5-131 group (T_X) and Control Group (C) vs T. (B) Venn Diagram of C vs T and T vs T_TX (C) Gene ontology (GO) enrichment plot in T vs C and T vs T_X groups. (D) Heatmap of Differential gene, identified Pebp1 as a potential mediator (E) IF staining of Pebp1 and quantification in different mice groups (4 weeks and 8 weeks, n = 6). Scale bars, 50 μm (E).

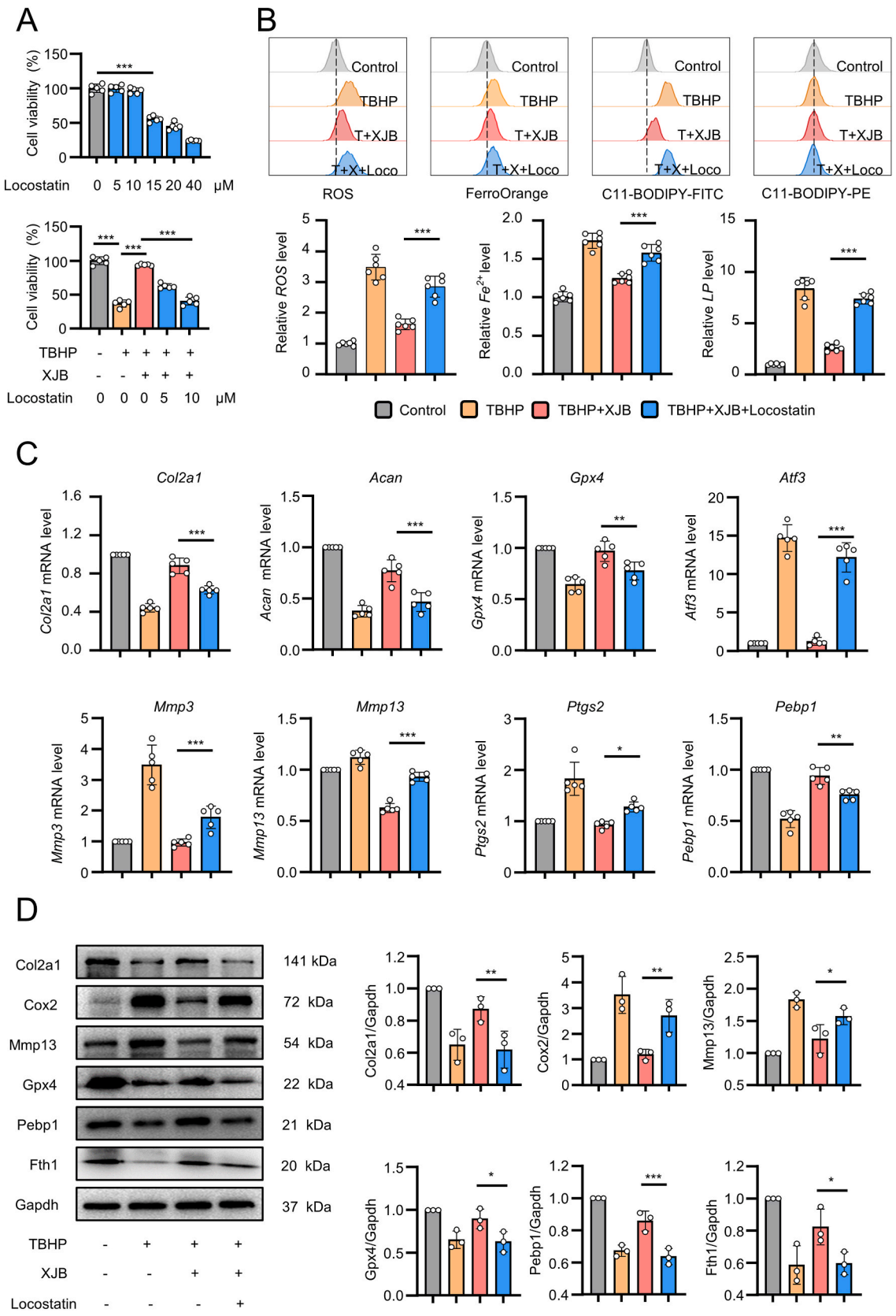

Fig. 5. Inhibition of pebp1 disables XJB-5-131 resistance to chondrocyte ferroptosis. (A) The viability of primary chondrocytes after Locostatin treatment with or without TBHP and XJB-5-131(n = 5). (B) Flow cytometry analysis and quantitative analysis of intracellular ROS, FerroOrange (Fe^{2+}), lipid peroxidation (C11-BODIPY) in different groups(n = 6). (C) Q-PCR analysis of indicated genes in chondrocytes treated with TBHP, TBHP + XJB-5-131 and TBHP + XJB-5-131+Locostatin for 6 h (n = 5). (D)Western blot analysis of protein expression and quantification of Col2a1, Cox2, MMP13, Fth1 and Gpx4 in different groups (n = 3). The values are presented as the means ± SDs. *P < 0.05; **P < 0.01; ***P < 0.001.

ferroptosis. We not only provided a potential possibility of modifying the pathological progression of OA but also indicated the direction for the subsequent application of XJB-5-131 as a ferroptosis inhibitor in other diseases. Nonetheless, there were several limitations in our study. OA was a multifactorial degenerative disease involving multiple cells and factors [52,53]. However, in this study, we only investigated the pathogenic mechanism of XJB-5-131 on ferroptosis in chondrocytes, while the studies on other cells (such as macrophage) and other pathogenic factors need to further studied. In addition, the pathological features of OA were degeneration of articular cartilage, hyperplasia of subchondral bone, osteogenesis at the joint edge, inflammation and proliferation of synovial tissue [54]. In our study, although we have provided microCT data of subchondral bone which is consistent with the pathological alleviation of OA, ferroptosis is related to bone homeostasis [55], and the specific mechanism of subchondral bone remodeling needs to be further explored.

5. Conclusion

In conclusion, we found that XJB-5-131 suppressed chondrocyte ferroptosis and alleviated OA progression by restoring Pebp1 expression. This work suggests XJB-5-131 as a potential therapeutic drug for exploring the disease-modifying drug of OA.

Funding

This research was funded by the National Natural Science Foundation of China (82172481, 32271409, 82302759, 82325035), Jiangsu Funding Program for Excellent Postdoctoral Talent (2022ZB753), Project funded by China Postdoctoral Science Foundation (2023M734292), the Fundamental Research Funds for the Central Universities (021414380528), Six Talent Peaks Project of Jiangsu Province (WSW-079), Innovation Project of National Orthopedics and Sports Medicine Rehabilitation Clinical Medical Research Center (2021-NCRC-CXJJ-ZH-16).

Declaration of competing interest

A conflict of interest occurs when an individual's objectivity is potentially compromised by a desire for financial gain, prominence, professional advancement or a successful outcome. The Editors of the *Journal of Orthopaedic Translation* strive to ensure that what is published in the Journal is as balanced, objective and evidence-based as possible. Since it can be difficult to distinguish between an actual conflict of interest and a perceived conflict of interest, the Journal requires authors to disclose all and any potential conflicts of interest.

Acknowledgements

All persons who have made substantial contributions to the work reported in the manuscript (e.g., technical help, writing and editing assistance, general support), but who do not meet the criteria for authorship, are named in the Acknowledgements and have given us their written permission to be named. If we have not included an Acknowledgements, then that indicates that we have not received substantial contributions from non-authors.

References

[1] Safiri S, Kolahi AA, Smith E, Hill C, Bettampadi D, Mansournia MA, et al. Global, regional and national burden of osteoarthritis 1990-2017: a systematic analysis of the Global Burden of Disease Study 2017. Ann Rheum Dis 2020;79(6):819–28.
[2] Yan J, Feng G, Ma L, Chen Z, Jin Q. Metformin alleviates osteoarthritis in mice by inhibiting chondrocyte ferroptosis and improving subchondral osteosclerosis and angiogenesis. J Orthop Surg Res 2022;17(1):333.
[3] Martel-Pelletier J, Barr AJ, Cicuttini FM, Conaghan PG, Cooper C, Goldring MB, et al. Osteoarthritis. Nat Rev Dis Prim 2016;2:16072.
[4] Hunter DJ, Bierma-Zeinstra S. Osteoarthritis. Lancet 2019;393(10182):1745–59.
[5] Latourte A, Kloppenburg M, Richette P. Emerging pharmaceutical therapies for osteoarthritis. Nat Rev Rheumatol 2020;16(12):673–88.
[6] Glyn-Jones S, Palmer AJ, Agricola R, Price AJ, Vincent TL, Weinans H, et al. Osteoarthritis. Lancet 2015;386(9991):376–87.
[7] Li X, Zhen Z, Tang G, Zheng C, Yang G. MiR-29a and MiR-140 protect chondrocytes against the anti-proliferation and cell matrix signaling changes by IL-1beta. Mol Cell 2016;39(2):103–10.
[8] Charlier E, Relic B, Deroyer C, Malaise O, Neuville S, Collee J, et al. Insights on molecular mechanisms of chondrocytes death in osteoarthritis. Int J Mol Sci 2016;17(12):2146.
[9] An S, Hu H, Li Y, Hu Y. Pyroptosis plays a role in osteoarthritis. Aging Dis 2020;11(5):1146–57.
[10] Yao X, Sun K, Yu S, Luo J, Guo J, Lin J, et al. Chondrocyte ferroptosis contribute to the progression of osteoarthritis. J Orthop Translat 2021;27:33–43.
[11] Dixon SJ, Lemberg KM, Lamprecht MR, Skouta R, Zaitsev EM, Gleason CE, et al. Ferroptosis: an iron-dependent form of nonapoptotic cell death. Cell 2012;149(5):1060–72.
[12] Tang D, Chen X, Kang R, Kroemer G. Ferroptosis: molecular mechanisms and health implications. Cell Res 2021;31(2):107–25.
[13] Jiang X, Stockwell BR, Conrad M. Ferroptosis: mechanisms, biology and role in disease. Nat Rev Mol Cell Biol 2021;22(4):266–82.
[14] Lv M, Cai Y, Hou W, Peng K, Xu K, Lu C, et al. The RNA-binding protein SND1 promotes the degradation of GPX4 by destabilizing the HSPA5 mRNA and suppressing HSPA5 expression, promoting ferroptosis in osteoarthritis chondrocytes. Inflamm Res 2022;71(4):461–72.
[15] Lv Z, Han J, Li J, Guo H, Fei Y, Sun Z, et al. Single cell RNA-seq analysis identifies ferroptotic chondrocyte cluster and reveals TRPV1 as an anti-ferroptotic target in osteoarthritis. EBioMedicine 2022;84:104258.
[16] Zhang S, Xu J, Si H, Wu Y, Zhou S, Shen B. The role played by ferroptosis in osteoarthritis: evidence based on iron dyshomeostasis and lipid peroxidation. Antioxidants 2022;11(9):1668.
[17] Miao Y, Chen Y, Xue F, Liu K, Zhu B, Gao J, et al. Contribution of ferroptosis and GPX4's dual functions to osteoarthritis progression. EBioMedicine 2022;76:103847.
[18] Macias CA, Chiao JW, Xiao J, Arora DS, Tyurina YY, Delude RL, et al. Treatment with a novel hemigramicidin-TEMPO conjugate prolongs survival in a rat model of lethal hemorrhagic shock. Ann Surg 2007;245(2):305–14.
[19] Xun Z, Rivera-Sanchez S, Ayala-Pena S, Lim J, Budworth H, Skoda EM, et al. Targeting of XJB-5-131 to mitochondria suppresses oxidative DNA damage and motor decline in a mouse model of Huntington's disease. Cell Rep 2012;2(5):1137–42.
[20] Escobales N, Nunez RE, Jang S, Parodi-Rullan R, Ayala-Pena S, Sacher JR, et al. Mitochondria-targeted ROS scavenger improves post-ischemic recovery of cardiac function and attenuates mitochondrial abnormalities in aged rats. J Mol Cell Cardiol 2014;77:136–46.
[21] Polyzos A, Holt A, Brown C, Cosme C, Wipf P, Gomez-Marin A, et al. Mitochondrial targeting of XJB-5-131 attenuates or improves pathophysiology in HdhQ150 animals with well-developed disease phenotypes. Hum Mol Genet 2016;25(9):1792–802.
[22] Polyzos AA, Wood NI, Williams P, Wipf P, Morton AJ, McMurray CT. XJB-5-131-mediated improvement in physiology and behaviour of the R6/2 mouse model of Huntington's disease is age- and sex- dependent. PLoS One 2018;13(4):e0194580.
[23] Zhao Z, Wu J, Xu H, Zhou C, Han B, Zhu H, et al. XJB-5-131 inhibited ferroptosis in tubular epithelial cells after ischemia-reperfusion injury. Cell Death Dis 2020;11(8):629.
[24] Krainz T, Gaschler MM, Lim C, Sacher JR, Stockwell BR, Wipf P. A mitochondrial-targeted nitroxide is a potent inhibitor of ferroptosis. ACS Cent Sci 2016;2(9):653–9.
[25] Gosset M, Berenbaum F, Thirion S, Jacques C. Primary culture and phenotyping of murine chondrocytes. Nat Protoc 2008;3(8):1253–60.
[26] Lv Z, Xu X, Sun Z, Yang YX, Guo H, Li J, et al. TRPV1 alleviates osteoarthritis by inhibiting M1 macrophage polarization via Ca(2+)/CaMKII/Nrf2 signaling pathway. Cell Death Dis 2021;12(6):504.
[27] Xu Z, Chen T, Luo J, Ding S, Gao S, Zhang J. Cartilaginous metabolomic study reveals potential mechanisms of osteophyte formation in osteoarthritis. J Proteome Res 2017;16(4):1425–35.
[28] Yeung K, Seitz T, Li S, Janosch P, McFerran B, Kaiser C, et al. Suppression of Raf-1 kinase activity and MAP kinase signalling by RKIP. Nature 1999;401(6749):173–7.
[29] Rudnitskaya AN, Eddy NA, Fenteany G, Gascon JA. Recognition and reactivity in the binding between Raf kinase inhibitor protein and its small-molecule inhibitor locostatin. J Phys Chem B 2012;116(34):10176–81.
[30] Ma J, Qiu Y, Wang M, Zhang M, Zhao X, Jiang H. Locostatin alleviates liver fibrosis induced by carbon tetrachloride in mice. Dig Dis Sci 2019;64(9):2570–80.
[31] Hu Z, Zhang H, Yang SK, Wu X, He D, Cao K, et al. Emerging role of ferroptosis in acute kidney injury. Oxid Med Cell Longev 2019;2019:8010614.
[32] Xu S, He Y, Lin L, Chen P, Chen M, Zhang S. The emerging role of ferroptosis in intestinal disease. Cell Death Dis 2021;12(4):289.
[33] Hong M, Rong J, Tao X, Xu Y. The emerging role of ferroptosis in cardiovascular diseases. Front Pharmacol 2022;13:822083.
[34] Chang S, Tang M, Zhang B, Xiang D, Li F. Ferroptosis in inflammatory arthritis: a promising future. Front Immunol 2022;13:955069.
[35] Kot K, Kosik-Bogacka D, Zietek P, Karaczun M, Ciosek Z, Lanocha-Arendarczyk N. Impact of varied factors on iron, nickel, molybdenum and vanadium concentrations in the knee joint. Int J Environ Res Publ Health 2020;17(3):813.

[36] Kocpinar EF, Gonul Baltaci N, Ceylan H, Kalin SN, Erdogan O, Budak H. Effect of a prolonged dietary iron intake on the gene expression and activity of the testicular antioxidant defense system in rats. Biol Trace Elem Res 2020;195(1):135–41.
[37] Sun K, Guo Z, Hou L, Xu J, Du T, Xu T, et al. Iron homeostasis in arthropathies: from pathogenesis to therapeutic potential. Ageing Res Rev 2021;72:101481.
[38] Theil EC. Iron, ferritin, and nutrition. Annu Rev Nutr 2004;24:327–43.
[39] Yang WS, Stockwell BR. Synthetic lethal screening identifies compounds activating iron-dependent, nonapoptotic cell death in oncogenic-RAS-harboring cancer cells. Chem Biol 2008;15(3):234–45.
[40] Dowdle WE, Nyfeler B, Nagel J, Elling RA, Liu S, Triantafellow E, et al. Selective VPS34 inhibitor blocks autophagy and uncovers a role for NCOA4 in ferritin degradation and iron homeostasis in vivo. Nat Cell Biol 2014;16(11):1069–79.
[41] Mancias JD, Wang X, Gygi SP, Harper JW, Kimmelman AC. Quantitative proteomics identifies NCOA4 as the cargo receptor mediating ferritinophagy. Nature 2014;509(7498):105–9.
[42] Wenzel SE, Tyurina YY, Zhao J, St Croix CM, Dar HH, Mao G, et al. PEBP1 wardens ferroptosis by enabling lipoxygenase generation of lipid death signals. Cell 2017;171(3):628–41.
[43] Anthonymuthu TS, Tyurina YY, Sun WY, Mikulska-Ruminska K, Shrivastava IH, Tyurin VA, et al. Resolving the paradox of ferroptotic cell death: ferrostatin-1 binds to 15LOX/PEBP1 complex, suppresses generation of peroxidized ETE-PE, and protects against ferroptosis. Redox Biol 2021;38:101744.
[44] Lamade AM, Wu L, Dar HH, Mentrup HL, Shrivastava IH, Epperly MW, et al. Inactivation of RIP3 kinase sensitizes to 15LOX/PEBP1-mediated ferroptotic death. Redox Biol 2022;50:102232.
[45] Su Y, Zhao D, Jin C, Li Z, Sun S, Xia S, et al. Dihydroartemisinin induces ferroptosis in HCC by promoting the formation of PEBP1/15-LO. Oxid Med Cell Longev 2021;2021:3456725.
[46] Zhao C, Sun G, Li Y, Kong K, Kan T, Yang F, et al. Forkhead box O3 attenuates osteoarthritis by suppressing ferroptosis through inactivation of NF-κB/MAPK signaling. J Orthop Translat 2023;39:147–62.
[47] Wan Y, Shen K, Yu H, Fan W. Baicalein limits osteoarthritis development by inhibiting chondrocyte ferroptosis. Free Radic Biol Med 2023;196:108–20.
[48] Paul BT, Manz DH, Torti FM, Torti SV. Mitochondria and Iron: current questions. Expert Rev Hematol 2017;10(1):65–79.
[49] Dan Dunn J, Alvarez LA, Zhang X, Soldati T. Reactive oxygen species and mitochondria: a nexus of cellular homeostasis. Redox Biol 2015;6:472–85.
[50] Barrera G, Gentile F, Pizzimenti S, Canuto RA, Daga M, Arcaro A, et al. Mitochondrial dysfunction in cancer and neurodegenerative diseases: spotlight on fatty acid oxidation and lipoperoxidation products. Antioxidants 2016;5(1):7.
[51] Rodriguez-Graciani KM, Chapa-Dubocq XR, Ayala-Arroyo EJ, Chaves-Negron I, Jang S, Chorna N, et al. Effects of ferroptosis on the metabolome in cardiac cells: the role of glutaminolysis. Antioxidants 2022;11(2):278.
[52] Zhang W, Robertson WB, Zhao J, Chen W, Xu J. Emerging trend in the pharmacotherapy of osteoarthritis. Front Endocrinol 2019;10:431.
[53] Zhang W, Ouyang H, Dass CR, Xu J. Current research on pharmacologic and regenerative therapies for osteoarthritis. Bone Res 2016;4:15040.
[54] Chen D, Shen J, Zhao W, Wang T, Han L, Hamiltin JL, et al. Osteoarthritis: toward a comprehensive understanding of pathological mechanism. Bone Res 2017;5:16044.
[55] Xiong Y, Chen L, Lin Z, Hu Y, Panayi AC, Zhou W, et al. The regulatory role of ferroptosis in bone homeostasis. Stem Cell Int 2022;2022:3568597.